ACS Energy LETTERS

http://pubs.acs.org/journal/aelccp

Detrimental Effects of Monoethanolamine and Other Amine-Based Capture Agents on the Electrochemical Reduction of CO_2

John Safipour, Adam Z. Weber, and Alexis T. Bell*

Cite This: *ACS Energy Lett.* 2023, 8, 5012–5017

Read Online

ACCESS | Metrics & More | Article Recommendations | Supporting Information

ABSTRACT: Reactive carbon capture (RCC) is a promising solution for carbon capture and utilization. RCC involves CO_2 capture, typically with amine solutions to form carbamate, followed by immediate conversion into value-added chemicals and fuels, typically via electrochemical means. RCC may enhance CO_2 reduction (CO_2R) by overcoming the inherent limiting low solubility of CO_2 in aqueous solutions. In this work, we present a systematic study of the influence of monoethanolamine (MEA) on CO_2R performance over an Ag cathode in $KHCO_3$ electrolytes. Contrary to prior work, the study finds no evidence for the direct reduction of carbamate anions. Instead, the presence of MEA suppresses the rate of CO formation while increasing that of H_2. These results are supported by a boundary-layer continuum model of mass transport and reaction that correctly predicts experimental trends and demonstrates that MEA reduces the concentration of CO_2 near the cathode. Thus, alternative strategies are necessary to achieve RCC in aqueous environments.

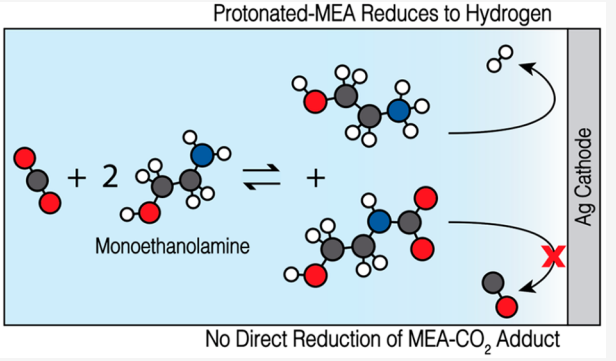

Carbon capture and utilization by means of electrochemical CO_2 reduction (CO_2R) to fuels and chemicals offer an attractive approach for reutilizing the carbon content in CO_2 released from stationary sources or captured from the atmosphere.[1−4] One of the serious limitations of CO_2R in aqueous solutions is the solubility of CO_2, which is ∼34 mM for 1 atm of gaseous CO_2 or even lower in an electrolyte due to salting out.[5,6] The low solubility of CO_2 combined with its low diffusion coefficient means that CO_2R becomes mass-transfer-limited at even low current densities (>10 mA/cm^2) in aqueous electrolyzers.[7−9] This limitation has led researchers to consider reactive carbon capture (RCC) as an alternative, where the addition of a carbon-capture agent to the electrolyte produces an adduct that can achieve higher concentrations than dissolved CO_2[10−17] and, ideally, the adduct would be amenable to electrochemical reduction at similar or enhanced rates compared to dissolved CO_2.

Several recent studies have suggested that RCC could be achieved by adding an amine to form a carbamate via[18,19]

$$CO_2 + 2RNH_2 \overset{K_C}{\rightleftharpoons} RNHCOO^- + RNH_3^+ \quad (1)$$

While the capture agent increases the total concentration of dissolved carbonaceous species, the question remains whether the resulting carbamate ($RNHCOO^-$) can be directly reduced to products. Differing conclusions have been reached on this point. Chen et al. first reported CO_2R over planar metal electrodes from an industrial, 30 wt % monoethanolamine (MEA) capture solution, noting that the carbamate and ammonium (RNH_3^+) ions act as a supporting electrolyte.[15] The CO_2R performance from the capture medium was enhanced with a porous electrode and the addition of a cationic surfactant, but the authors note that it is likely only aqueous CO_2 participates in reduction. Lee et al. reported the conversion of MEA-CO_2 to CO over an Ag electrocatalyst with a Faradaic efficiency of 72% at 60 °C and a current density of 50 mA/cm^2 from a 30 wt % MEA/2 M KCl solution.[16] The solution was purged with N_2 before electrolysis to remove aqueous CO_2 as a source for CO evolution; furthermore, the authors suggest that the alkali cations in the electrochemical double layer facilitate the reduction of the carbamate adduct, since they observe poorer performance from an MEA solution without KCl. On the other hand, Shen et al. investigated CO_2

Received: September 16, 2023
Revised: October 23, 2023
Accepted: November 2, 2023
Published: November 6, 2023

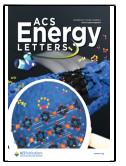

https://doi.org/10.1021/acsenergylett.3c01953
ACS Energy Lett. 2023, 8, 5012−5017

electrolysis in ammonium carbamate and CO_2-saturated MEA solutions using a rotating Ag cylinder to achieve well-defined mass transport to the cathode.[17,20] Their work shows that CO is derived primarily from dissolved CO_2 and that carbamate reduction occurs only at highly negative cathode potentials. These findings are supported by DFT calculations for the ammonium carbamate system, which suggests that the existence of a relatively stable surface-bound NH_2COOH species limits the rate of C−N bond cleavage necessary for direct reduction of the carbamate.

In this work, we seek to establish whether carbamates can be directly reduced by an Ag foil electrocatalyst in aqueous systems via

$$RNHCOO^- + 2H_2O + 2e^- \rightarrow RNH_2 + CO + 3OH^- \quad (2)$$

Monoethanolamine (MEA, R corresponds to $-CH_2CH_2OH$ and K_C has a value of 6.77×10^4 in eq 1) was used for all the experiments because it is water-soluble and forms a particularly stable carbamate and the thermodynamic and kinetic properties of MEA solutions have been most studied in the literature.[21−23] We have carried out a systematic study of CO_2R over an Ag cathode in an aqueous solution of $KHCO_3$ containing MEA. Our experimental results are supported with a continuum model of mass transport and reaction in the mass-transfer boundary layer.

Electrochemical CO_2 reduction (CO_2R) was performed using an aqueous electrochemical compression cell machined from polyether ether ketone (PEEK). Prior to each experiment, the cell components were cleaned by sonicating them in 10 wt % nitric acid. The cell compartments were separated by an anion-exchange membrane (PiperION-A80-HCO3, Versogen). Silver foil (99.998%, 0.1 mm thick, Thermo Fisher Scientific) was used as the cathode, which was mechanically polished (400 grit), thoroughly rinsed in deionized (DI) water, and sonicated in acetone (≥99.5%, Sigma-Aldrich) prior to each experiment.[24] The anode was a platinum mesh (99.995%, Sigma-Aldrich). The working electrode and counter electrode had geometric areas of 0.5 and 2 cm^2, respectively (Figure S1). For the three-electrode configuration, a Ag/AgCl reference electrode (filled with 3.4 M KCl, Leak-Free, Innovative Instruments) was used. The potassium bicarbonate ($KHCO_3$, 99.7%, Sigma-Aldrich) and monoethanolamine (MEA, ≥99.0%, Sigma-Aldrich) electrolyte solutions were prepared with Milli-Q water and pretreated with a chelating agent (Chelex 100, Na form, 50−100 mesh (dry), Sigma-Aldrich) to eliminate metallic impurities.

The catholyte was saturated with CO_2 (25 sccm, 99.999%, Airgas) for 1.5 h in a reservoir before each experiment, then circulated through the compression cell at a rate of 80 mL/min using a peristaltic pump while continuously sparging CO_2 into the solution. Electrochemical chronoamperometry experiments were conducted using a potentiostat (BioLogic VSP-300). The uncompensated resistance was determined by the current interrupt method and was compensated to 85% with the potentiostat.[25] To analyze the CO_2 reduction products, an online gas chromatograph (multiple gas analyzer #5, SRI Instruments) equipped with both Hayesep D and Molsieve 5A columns and both thermal-conductivity and flame-ionization detectors was employed.

The equilibrium distribution of species in the $KHCO_3$-MEA-CO_2 electrolyte was calculated assuming equilibration with a reservoir of gaseous CO_2 at a partial pressure of 1 atm. A system of equations consisting of seven equilibrium reactions, one mass balance (conservation of MEA and its derivatives), and one charge balance (electroneutrality) was solved in MATLAB to determine the concentration of the nine reacting species (see Supporting Information section S2 for details and relevant constants provided in Tables S1 and S2). The activity of ions was calculated using the Davies equation, and while this approach does not consider ion-specific interactions, it is superior to neglecting the effect of ionic strength on the activity of charged species. The activity of aqueous CO_2 is given by the Weisenberger−Schumpe model,[5] and the activity of water is assumed to be unity for all electrolyte concentrations.

A one-dimensional model (solved in COMSOL Multiphysics 6.1) was used to predict concentration profiles for nine species present in the mass-transfer boundary layer. It was assumed that beyond the boundary layer the species' concentrations are governed by the bulk solution thermodynamics.[7] A diagram of the modeled system is depicted in Figure S3; details of the model are given in section S3 of the Supporting Information, and relevant kinetic and diffusion constants are provided in Tables S3−S5. Electrode reactions are assumed to follow concentration-dependent Tafel kinetics. For an electrochemical system subject to significant mass-transport limitations, kinetic parameters (exchange current density, transfer coefficient, and boundary-layer thickness) are obtained by a least-squares fit to the data using the BOBYQA algorithm, an approach similar to that described by Corpus et al.[26] Further details of the parameter-determination procedure are shown in Figures S4−S6.

Figure 1 shows that the addition of MEA to 0.1 M $KHCO_3$ has a significant impact on the partial current densities (PCDs) of H_2 and CO. The H_2 PCD increases with an increasing MEA concentration (Figure 1a), whereas the CO PCD decreases (Figure 1b). These changes can be partially attributed to the increase in bulk HCO_3^- concentration resulting from the presence of MEA (see Table 1), since HCO_3^- is known to act as a proton donor for hydrogen-evolution reaction (HER) because it has a lower pK_a than H_2O.[27−29] However, Table 1 also shows that addition of MEA to 1.0 M $KHCO_3$ does not change the HCO_3^- concentration; this solution still shows an increase in H_2 PCD upon the addition of MEA (Figure 2a). This observation suggests that monoethanolammonium ($MEAH^+$), which is present in substantial concentrations in the bulk electrolyte, can act as a tertiary proton source for hydrogen evolution in an alkaline electrolyte. This reasoning is supported by the recognition that the pK_a of $MEAH^+$ is 9.44, which is lower than that of water (14.0) and HCO_3^- (10.3). Hence, $MEAH^+$ can serve as an effective proton donor at concentrations that are significantly lower than those of water and HCO_3^-. This interpretation is supported by our simulation discussed below.

The CO PCD in MEA-containing electrolyte never exceeds that obtained from an MEA-free electrolyte, strongly suggesting that direct carbamate reduction does not occur (Figures 1b, 2b, and S2b). If this CO-evolution reaction (COER) pathway were possible, we would expect a greater rate of CO production from the MEA-containing electrolyte, corresponding to a higher effective concentration of reducible, carbon-containing species. This result holds for the case of 1.0 M $KHCO_3$ electrolyte with 0.2 M MEA additive, which contains carbamate anions at a concentration 4.4 times that of free CO_2 dissolved in the bulk (Table 1, Figure 2b). What we

https://doi.org/10.1021/acsenergylett.3c01953
ACS Energy Lett. 2023, 8, 5012−5017

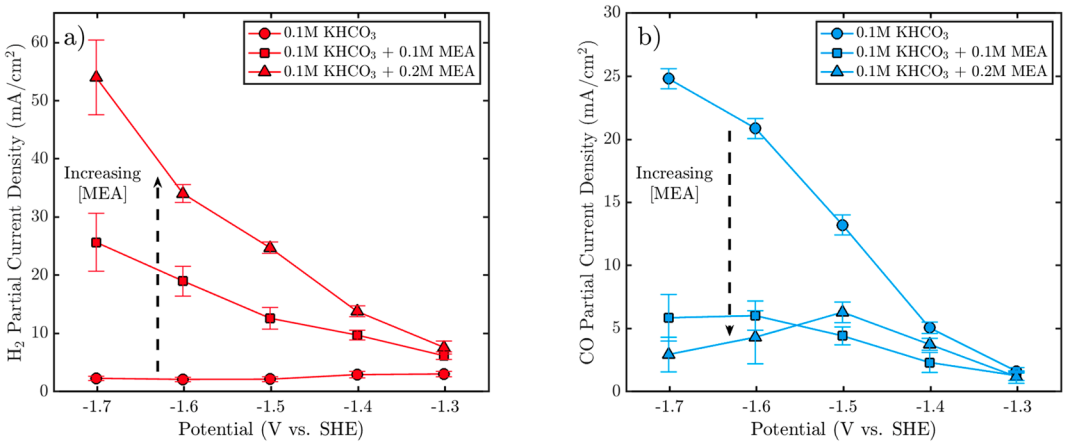

Figure 1. Measured (a) hydrogen and (b) carbon monoxide partial current densities with catholytes containing 0.1 M potassium bicarbonate and varied concentrations of MEA. The solutions containing 0.1 and 0.2 M MEA additive perform noticeably worse than the amine-free control.

Table 1. Results of Thermodynamic Speciation Modeling with Amine-Capture Equilibrium Constants from Fernandes et al.[22,a]

	electrolyte composition			
	0.1 M $KHCO_3$	0.1 M $KHCO_3$ + 0.2 M MEA	1.0 M $KHCO_3$	1.0 M $KHCO_3$ + 0.2 M MEA
$[CO_2]_{aq}$	32.7 mM	31.2 mM	23.8 mM	23.4 mM
$[HCO_3^-]$	0.100 M	0.271 M	0.990 M	0.997 M
$[MEAH^+]$		182 mM		94.8 mM
[carbamate]		16.8 mM		103 mM

[a]Notably, the 1.0 M potassium bicarbonate electrolyte with 0.2 M MEA additive contains carbamate at 103 mM, which is a factor of 4.4 greater than the free CO_2 concentration.

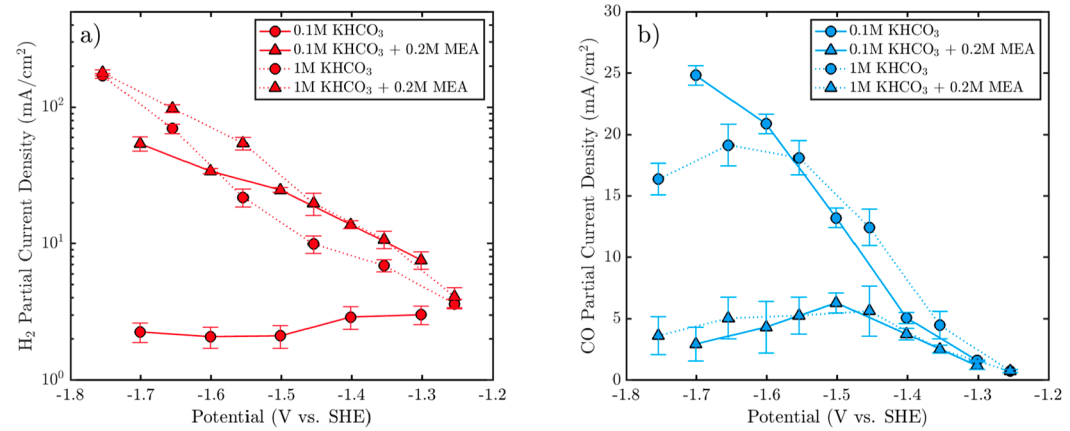

Figure 2. Comparison of (a) hydrogen and (b) carbon monoxide partial current density between solutions of 0.1 and 1.0 M potassium bicarbonate, with and without 0.2 M MEA. Despite a significant carbamate concentration (103 mM) in the 1.0 M $KHCO_3$ + 0.2 M MEA solution, the CO partial current density is far less than that from the untreated 1.0 M $KHCO_3$ electrolyte, suggesting no direct conversion of carbamate.

observe instead is a significant reduction in CO PCD in MEA-containing electrolyte. While it is possible that MEA and its derivatives affect the electrochemical double layer or strongly adsorb to the silver cathode, thereby inhibiting CO evolution, we hypothesize, instead, that MEA affects the solution chemistry near the cathode, reducing the local CO_2 concentration and CO PCD as a result. To support this hypothesis, we examined the effects of chemical transport and reaction in the mass-transfer boundary layer near the cathode using a 1D continuum model.

Figure 3 shows that the 1D continuum model correctly predicts the H_2 and CO PCDs observed with 0.1 M $KHCO_3$ with 0, 0.1, and 0.2 M concentrations of MEA. Similar results for the 1.0 M $KHCO_3$ electrolyte with MEA are presented in Figure S8. To capture the effect of MEA addition on H_2 formation, it is necessary to include in the model an electrode reaction for H_2 generation from $MEAH^+$,

$$2MEAH^+ + 2e^- \rightarrow H_2 + 2MEA \quad (3)$$

and the kinetics of the reaction between MEA, released in the above HER pathway, with dissolved CO_2 to produce

https://doi.org/10.1021/acsenergylett.3c01953
ACS Energy Lett. 2023, 8, 5012−5017

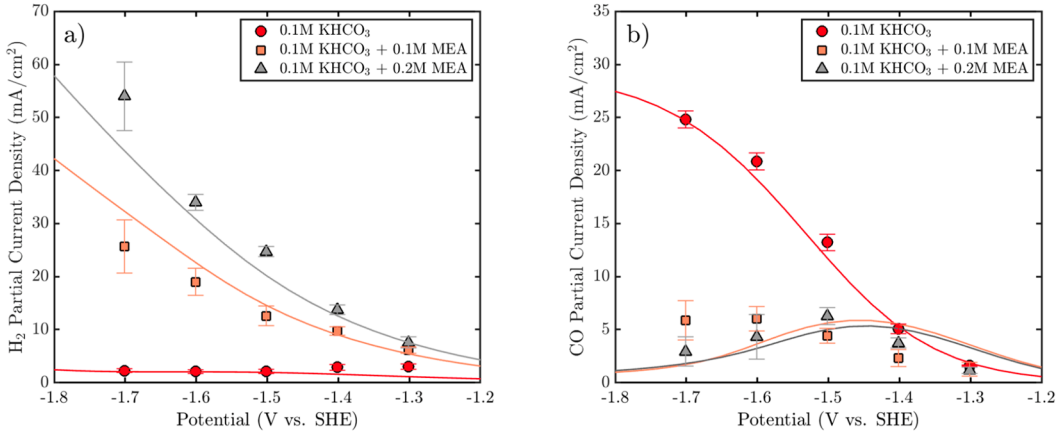

Figure 3. Comparison between experimental (points) and model (lines) for (a) hydrogen and (b) carbon monoxide partial current densities evolved from 0.1 M $KHCO_3$ electrolyte with varying concentrations of MEA.

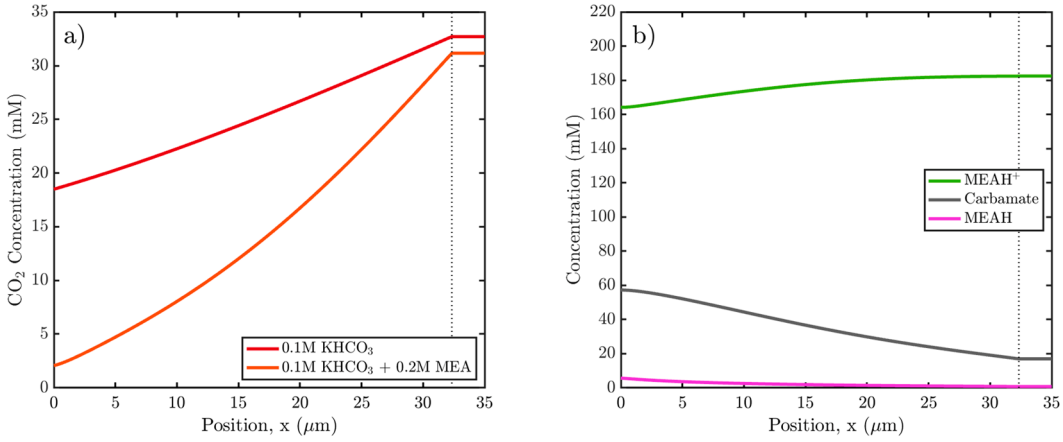

Figure 4. Simulated boundary-layer concentration profiles at an applied potential of −1.5 V vs SHE, where the zero coordinate corresponds to the Ag cathode surface. (a) Comparison of the dissolved CO_2 concentration profile in 0.1 M $KHCO_3$ electrolyte with and without 0.2 M MEA additive. (b) MEA, $MEAH^+$, and carbamate concentration profiles in 0.1 M $KHCO_3$ + 0.2 M MEA electrolyte, showing the depletion of $MEAH^+$ and accumulation of MEA and carbamate relative to their respective bulk values. Carbamate concentration is elevated due to the reaction of locally generated MEA with aqueous CO_2, causing the result in (a).

carbamate anions (eq 1). Inclusion of these processes provides a reasonably good description of the effect of low concentrations of MEA on the rate of CO formation in $KHCO_3$ solutions. The enhanced production of H_2 by MEA is predicted by the model and is consistent with the two arguments discussed previously: (1) MEA elevates the concentration of HCO_3^- and associated HCO_3^--derived HER rate and (2) MEAH+ is directly reduced to H_2. Furthermore, the model fails to correctly describe the H_2 PCD when eq 2 is not incorporated (Figure S7). To understand how MEA suppresses the production of CO, it is instructive to examine the species concentration profiles within the mass-transfer boundary layer, which are shown in Figure 4.

The model provides insight into the suppression of the CO PCD when MEA is added to the electrolyte. Specifically, it predicts a lower concentration of dissolved CO_2 in the boundary layer for a given cathode potential when MEA is present, thereby explaining the reduction in the CO evolution rate observed experimentally given that CO evolution is well-modeled by concentration-dependent Tafel kinetics (Figure 4a). In MEA-free electrolyte, the decrease in CO_2 concentration relative to its bulk concentration is well-known to occur through a combination of CO_2 reduction at the cathode and homogeneous reaction with OH^- anions, generated by HER and COER, with dissolved CO_2.[7] In the MEA-containing electrolyte, CO_2 is further depleted by reaction with MEA released near the cathode, resulting in the formation of carbamate anions; Figure 4b shows that the concentration of MEA and carbamate anions in the boundary layer is higher than in the bulk electrolyte. Two pathways contribute to the local generation of MEA: (1) the electrochemical reduction of $MEAH^+$ to H_2 and (2) the dissociation of $MEAH^+$ due to the high local pH. Deprotonation of $MEAH^+$ occurs before that of HCO_3^- because it is relatively acidic (the pK_a of $MEAH^+$ is 9.44 while that of HCO_3^- is 10.3). Once again, it is important to note that despite a high concentration of carbamate anions at the cathode surface (57.2 mM, which exceeds the *bulk* concentration of CO_2), the CO PCD for the 0.1 M $KHCO_3$ MEA-containing electrolyte is much lower than that for MEA-free electrolyte (4.41 versus 13.0 mA/cm^2 at an applied potential of −1.5 V vs SHE). These observations strongly support the conclusion that carbamate anions do not undergo reduction.

In addition to demonstrating that direct carbamate anions do not undergo reduction, our analysis finds no evidence that elevated bulk concentrations of soluble carbon in the form of

https://doi.org/10.1021/acsenergylett.3c01953
ACS Energy Lett. 2023, 8, 5012−5017

MEA-bound CO_2 enhance continuous CO_2R operation. Furthermore, as shown in Figure S9, additional simulations with other amine species known to form stable carbamates spanning a range of binding strengths, K_C, from 1.95×10^3 to 1.42×10^6 and ammonium ion acidities, pK_a, from 8.49 to 11.14 show little or no improvement relative to what is observed for MEA. To explain the differences in H_2 and CO evolution rates for each amine-electrolyte, Table S6 contains the predicted bulk composition with comparison to the base-case MEA. In all cases the CO PCD is lower in the presence of the CO_2 capture agent than in its absence. We acknowledge that these simulations ignore the possibility of direct carbamate reduction and that further experimental work or theoretical calculations may suggest that a non-MEA carbamate is amenable to such a reaction pathway. However, the reduction of the ammonium species to H_2 negatively affects the CO Faradaic efficiency, making this approach unattractive even with potential carbamate reduction.

Our systematic study of the effect of MEA addition to an aqueous electrolyte on the electrochemical reduction of CO_2 reveals no evidence for direct reduction of carbamate anions formed by the reaction of CO_2 with MEA or for carbamate anions serving as reservoir of CO_2. In fact, MEA addition results in a high bulk concentration of $MEAH^+$, a species that simultaneously increases H_2 PCD and contributes to reduction of the CO PCD. A continuum model developed to interpret the experimental observations correctly describes the observed effects of MEA addition. The model confirms that $MEAH^+$ acts as a proton source for hydrogen evolution and that MEA reduces the local CO_2 concentration and consequently the CO PCD. Therefore, it is our recommendation that continued research into CO_2R considers only the reduction of CO_2 after thermal desorption from the amine-based adsorbate solution as opposed to in its captured state.

■ ASSOCIATED CONTENT

Supporting Information

The Supporting Information is available free of charge at https://pubs.acs.org/doi/10.1021/acsenergylett.3c01953.

Materials and methods, additional experimental data, and tabulated constants (PDF)

■ AUTHOR INFORMATION

Corresponding Author

Alexis T. Bell − *Department of Chemical and Biomolecular Engineering, University of California, Berkeley, California 94720, United States; Lawrence Berkeley National Laboratory, Berkeley, California 94720, United States;* orcid.org/0000-0002-5738-4645; Email: alexbell@berkeley.edu

Authors

John Safipour − *Department of Chemical and Biomolecular Engineering, University of California, Berkeley, California 94720, United States; Lawrence Berkeley National Laboratory, Berkeley, California 94720, United States*

Adam Z. Weber − *Lawrence Berkeley National Laboratory, Berkeley, California 94720, United States;* orcid.org/0000-0002-7749-1624

Complete contact information is available at: https://pubs.acs.org/10.1021/acsenergylett.3c01953

Notes

The authors declare no competing financial interest.

■ ACKNOWLEDGMENTS

This work was supported by a grant from the Office of the President of the University of California as well as an award (L22CR4468) from the National Laboratory Research Fees Program, which supports the Center for Direct Conversion of Captured CO_2 into Chemicals and Fuels. We also thank our collaborators in the Center for contributions to discussions which guided these efforts, including the senior investigators K. L. Abdul-Aziz, L. Berben, M. Findlater, C. Hahn, A. R. Kulkarni, G. Ménard, C. G. Morales-Guio, P. Sautet, and J. Y. Yang. Computational resources for this work were provided by the Molecular Graphics and Computation Facility at the UC Berkeley College of Chemistry, supported by the National Institutes of Health Grant NIH S10OD034382.

■ REFERENCES

(1) Resasco, J.; Bell, A. T. Electrocatalytic CO_2 Reduction to Fuels: Progress and Opportunities. *Trends Chem.* **2020**, *2*, 825−836.

(2) Garg, S.; Li, M.; Weber, A. Z.; Ge, L.; Li, L.; Rudolph, V.; Wang, G.; Rufford, T. E. Advances and Challenges in Electrochemical CO_2 Reduction Processes: An Engineering and Design Perspective Looking Beyond New Catalyst Materials. *J. Mater. Chem. A* **2020**, *8*, 1511−1544.

(3) Nitopi, S.; Bertheussen, E.; Scott, S. B.; Liu, X.; Engstfeld, A. K.; Horch, S.; Seger, B.; Stephens, I. E. L.; Chan, K.; Hahn, C.; Nørskov, J. K.; Jaramillo, T. F.; Chorkendorff, I. Progress and Perspectives of Electrochemical CO_2 Reduction on Copper in Aqueous Electrolyte. *Chem. Rev.* **2019**, *119*, 7610−7672.

(4) Hori, Y.; Kikuchi, K.; Suzuki, S. Production of CO and CH4 in Electrochemical Reduction of CO2 at Metal Electrodes in Aqueous Hydrogencarbonate Solution. *Chem. Lett.* **1985**, *14* (11), 1695−1698.

(5) Weisenberger, S.; Schumpe, A. Estimation of Gas Solubilities in Salt Solutions at Temperatures from 273 to 363 K. *AIChE J.* **1996**, *42* (1), 298−300.

(6) Pabsch, D.; Held, C.; Sadowski, G. Modeling the CO2 Solubility in Aqueous Electrolyte Solutions Using EPC-SAFT. *J. Chem. Eng. Data* **2020**, *65* (12), 5768−5777.

(7) Gupta, N.; Gattrell, M.; MacDougall, B. Calculation for the Cathode Surface Concentrations in the Electrochemical Reduction of CO_2 in $KHCO_3$ Solutions. *J. Appl. Electrochem.* **2006**, *36*, 161−172.

(8) Singh, M. R.; Clark, E. L.; Bell, A. T. Effects of Electrolyte, Catalyst, and Membrane Composition and Operating Conditions on the Performance of Solar-Driven Electrochemical Reduction of Carbon Dioxide. *Phys. Chem. Chem. Phys.* **2015**, *17*, 18924−18936.

(9) Clark, E. L.; Resasco, J.; Landers, A.; Lin, J.; Chung, L.-T.; Walton, A.; Hahn, C.; Jaramillo, T. F.; Bell, A. T. Standards and Protocols for Data Acquisition and Reporting for Studies of the Electrochemical Reduction of Carbon Dioxide. *ACS Catal.* **2018**, *8*, 6560−6570.

(10) Li, M.; Yang, K.; Abdinejad, M.; Zhao, C.; Burdyny, T. Advancing integrated CO_2 electrochemical conversion with amine-based CO_2 capture: a review. *Nanoscale* **2022**, *14*, 11892−11908.

(11) Siegel, R. E.; Pattanayak, S.; Berben, L. A. Reactive Capture of CO2: Opportunities and Challenges. *ACS Catal.* **2023**, *13* (1), 766−784.

(12) Jerng, S. E.; Gallant, B. M. Electrochemical Reduction of CO2 in the Captured State Using Aqueous or Nonaqueous Amines. *iScience* **2022**, *25* (7), 104558.

(13) Sullivan, I.; Goryachev, A.; Digdaya, I. A.; Li, X.; Atwater, H. A.; Vermaas, D. A.; Xiang, C. Coupling Electrochemical CO2 Conversion with CO2 Capture. *Nature Catalysis* **2021**, *4* (11), 952−958.

(14) Pérez-Gallent, E.; Vankani, C.; Sánchez-Martínez, C.; Anastasopol, A.; Goetheer, E. Integrating CO2 Capture with

Electrochemical Conversion Using Amine-Based Capture Solvents as Electrolytes. *Ind. Eng. Chem. Res.* **2021**, *60* (11), 4269−4278.
(15) Chen, L.; Li, F.; Zhang, Y.; Bentley, C. L.; Horne, M.; Bond, A. M.; Zhang, J. Electrochemical Reduction of Carbon Dioxide in a Monoethanolamine Capture Medium. *ChemSusChem* **2017**, *10* (20), 4109−4118.
(16) Lee, G.; Li, Y. C.; Kim, J.-Y.; Peng, T.; Nam, D.-H.; Sedighian Rasouli, A.; Li, F.; Luo, M.; Ip, A. H.; Joo, Y.-C.; Sargent, E. H. Electrochemical Upgrade of CO2 from Amine Capture Solution. *Nature Energy* **2021**, *6*, 46−53.
(17) Shen, K.; Cheng, D.; Reyes-Lopez, E.; Jang, J.; Sautet, P.; Morales-Guio, C. G. On the Origin of Carbon Sources in the Electrochemical Upgrade of CO_2 from Carbon Capture Solutions. *Joule* **2023**, *7*, 1260−1276.
(18) Lillia, S.; Bonalumi, D.; Fosbøl, P. L.; Thomsen, K.; Jayaweera, I.; Valenti, G. Thermodynamic and Kinetic Properties of NH3-K2CO3-CO2-H2O System for Carbon Capture Applications. *International Journal of Greenhouse Gas Control* **2019**, *85*, 121−131.
(19) Zhu, K.; Yue, C.; Wei, Z.; Huang, J.; Hu, M.; Ji, Y.; Liu, H.; Zhu, H.; Guo, W.; Zhou, F.; Yao, C.; Huang, Y. Experimental and Thermodynamic Investigation on CO2 Absorption in Aqueous MEA Solutions. *Adv. Mater. Sci. Eng.* **2022**, *2022*, 6278342.
(20) Jang, J.; Rüscher, M.; Winzely, M.; Morales-Guio, C. G. Gastight Rotating Cylinder Electrode: Toward Decoupling Mass Transport and Intrinsic Kinetics in Electrocatalysis. *AIChE J.* **2022**, *68* (5), e17605.
(21) Wang, Y.; Zhao, L.; Otto, A.; Robinius, M.; Stolten, D. A Review of Post-Combustion CO_2 Capture Technologies from Coal-Fired Power Plants. *Energy Procedia* **2017**, *114*, 650−665.
(22) Fernandes, D.; Conway, W.; Burns, R.; Lawrance, G.; Maeder, M.; Puxty, G. Investigations of Primary and Secondary Amine Carbamate Stability by ^{1}H NMR Spectroscopy for Post Combustion Capture of Carbon Dioxide. *J. Chem.Thermo.* **2012**, *54*, 183−191.
(23) Boot-Handford, M. E.; Abanades, J. C.; Anthony, E. J.; Blunt, M. J.; Brandani, S.; Mac Dowell, N.; Fernández, J. R.; Ferrari, M.-C.; Gross, R.; Hallett, J. P.; Haszeldine, R. S.; Heptonstall, P.; Lyngfelt, A.; Makuch, Z.; Mangano, E.; Porter, R. T. J.; Pourkashanian, M.; Rochelle, G. T.; Shah, N.; Yao, J. G.; Fennell, P. S. Carbon Capture and Storage Update. *Energy Environ. Sci.* **2014**, *7*, 130−189.
(24) Hatsukade, T.; Kuhl, K. P.; Cave, E. R.; Abram, D. N.; Jaramillo, T. F. Insights into the Electrocatalytic Reduction of CO2 on Metallic Silver Surfaces. *Phys. Chem. Chem. Phys.* **2014**, *16* (27), 13814−13819.
(25) Kim, C.; Weng, L.-C.; Bell, A. T. Impact of Pulsed Electrochemical Reduction of CO2 on the Formation of C2+ Products over Cu. *ACS Catal.* **2020**, *10* (21), 12403−12413.
(26) Corpus, K. R. M.; Bui, J. C.; Limaye, A. M.; Pant, L. M.; Manthiram, K.; Weber, A. Z.; Bell, A. T. Coupling Covariance Matrix Adaptation with Continuum Modeling for Determination of Kinetic Parameters Associated with Electrochemical CO2 Reduction. *Joule* **2023**, *7* (6), 1289−1307.
(27) Resasco, J.; Lum, Y.; Clark, E.; Zeledon, J. Z.; Bell, A. T. Effects of Anion Identity and Concentration on Electrochemical Reduction of CO_2. *ChemElectroChem* **2018**, *5*, 1064.
(28) Marcandalli, G.; Goyal, A.; Koper, M. T. M. Electrolyte Effects on the Faradaic Efficiency of CO2 Reduction to CO on a Gold Electrode. *ACS Catal.* **2021**, *11* (9), 4936−4945.
(29) Kas, R.; Yang, K.; Yewale, G. P.; Crow, A.; Burdyny, T.; Smith, W. A. Modeling the Local Environment within Porous Electrode during Electrochemical Reduction of Bicarbonate. *Ind. Eng. Chem. Res.* **2022**, *61*, 10461−10473.

https://doi.org/10.1021/acsenergylett.3c01953
ACS Energy Lett. 2023, 8, 5012−5017